

# Shaping a Swarm With a Shared Control Input Using Boundary Walls and Wall Friction

Paper-ID [add your ID here]

**Abstract**—Micro- and nano-robots hold promise for targeted drug delivery and micro-scale manufacturing. Due to their small size, large numbers of micro-robots are required to deliver sufficient payloads, but their small size makes it difficult to perform onboard computation or contain a power and propulsion source. For this reason these robots are usually powered and controlled by global inputs, such as a uniform external electric or magnetic field, and every robot receives exactly the same control inputs. Nevertheless, these applications require precision control of the shape and position of the robot swarm. Precision control requires breaking the symmetry caused by the global input.

A promising technique uses collisions with boundary walls to shape the swarm, however, the range of configurations created by conforming a swarm to a boundary wall is limited. In this paper we described the set of stable configurations of a swarm in two canonical workspaces, a circle and a square.

To increase the diversity of configurations, we add wall friction to our model. We provide algorithms using friction with walls to place two robots at arbitrary locations in a rectangular workspace. Next, we extend this algorithm to place  $n$  robots at desired locations. We conclude with efficient techniques to control the variance of a swarm along directions not orthogonal to the boundary walls, something not possible without wall-friction. Hardware implementations with 97 robots, and simulations validate these results.

## I. INTRODUCTION

Micro- and nano-robots can be manufactured in large numbers, see recent examples in Donald et al. [1], Ghosh and Fischer [3], Kim et al. [6], or Martel et al. [8]. Our vision is for large swarms of robots remotely guided 1) through the human body, to cure disease, heal tissue, and prevent infection and 2) ex vivo to assemble structures in parallel. For each application, large numbers of micro robots are required to deliver sufficient payloads, but the small size of these robots makes it difficult to perform onboard computation. Instead, these robots are often controlled by a global, broadcast signal. The biggest barrier to this vision is a lack of control techniques that can reliably exploit large populations despite high under-actuation.

Even without obstacles or boundaries, the mean position of a swarm is controllable. By adding rectangular boundary walls, some higher-order moments such as the swarm's position variance orthogonal to the boundary walls ( $\sigma_x$  and  $\sigma_y$  for a workspace with axis-aligned walls) are also controllable. A limitation is that global control can only compress a swarm orthogonal to obstacles. One implication is that a swarm in an axis-aligned rectangular workspace can not generate a non-zero covariance. This limitation is detrimental to desired applications because the ability to orient the swarm is often useful for navigating narrow passages.

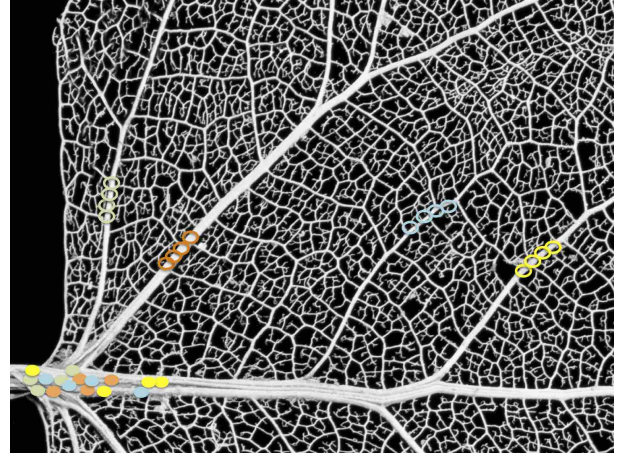


Fig. 1. Vascular networks are common in biology such as the circulatory system and cerebrospinal spaces, as well as in porous media including sponges and pumice stone. Navigating a swarm using global inputs, where each member receives the same control inputs, is challenging due to the many obstacles. This paper focuses on using boundary walls and wall friction to break the symmetry caused by the global input and control the shape of a swarm.

After a review of recent related work (Section II), this paper provides analytical position control results in two canonical workspaces with frictionless walls (Section III-A). These results are limited in the set of shapes that can be controlled. To extend the range of possible shapes, we introduce wall friction to the system model (Section III-B). We prove that two orthogonal boundaries with high friction are sufficient to arbitrarily position two robots (Section III-C), extend this proof to prove that a rectangular workspace with high friction boundaries is sufficient to position a swarm of  $n$  robots arbitrarily within a subset of the workspace (Section ), implement both position control algorithms in simulation and on a hardware setup with up to 97 robots (Sections IV and V), and end with directions for future research (Section ).

## II. RELATED WORK

Controlling the *shape*, or relative positions, of a swarm of robots is a key ability for a range of applications. Correspondingly, it has been studied from a control-theoretic perspective in both centralized and decentralized approaches. For examples of each, see the centralized virtual leaders in Egerstedt and Hu [2], and the gradient-based decentralized controllers using control-Lyapunov functions in Hsieh et al. [4]. However, most approaches assume a level of intelligence and autonomy in the individual robots that exceeds the capabilities of current

micro- and nano-robots such as those in Martel [7], Yan et al. [16].

Instead, this paper focuses on centralized techniques that apply the same control input to each member of the swarm. Precision control requires breaking the symmetry caused by the global input. The techniques in this paper are inspired by fluid-flow techniques and artificial force-fields.

a) *Shear forces*: are unaligned forces that push one part of a body in one direction, and another part of the body in the opposite direction. These shear forces are common in fluid flow along boundaries. Most introductory fluid dynamics textbooks provide models, for example, see Munson et al. [9]. Similarly, a swarm of robots under global control pushed along a boundary will experience shear forces. This is a position-dependent force, and so can be exploited to control the configuration or shape of the swarm. Physics-based swarm simulations have used these forces to disperse a swarm's spatial position for accomplishing coverage tasks Spears et al. [12].

b) *Artificial Force-fields*: Much research has focused on generating artificial force-fields that can be used to rearrange passive components. Applications have included techniques to design shear forces to a single object for sensorless manipulation Sudsang and Kavraki [13]. Vose et al. [14, 15] demonstrated a collection of 2D force fields generated by 6DOF vibration inputs to a rigid plate. This collection of force fields, including shear forces, could be used as a set of primitives for motion control for steering the formation of multiple objects.

### III. THEORY

#### A. Controlling Covariance: Fluid Settling In a Tank

One method to control the shape is to simply push the swarm in a given direction until the swarm conforms to the boundary.

c) *Square workplace*: This section examines the mean, variance, covariance and correlation of a very large swarm of robots as they move inside a square workplace under the influence of gravity pointing in the direction  $\beta$ . The swarm is large, but the robots are small in comparison, and together cover an area of constant volume  $A$ . Under a global input such as gravity, they flow like water, moving to a side of the workplace and forming a polygonal shape.

The range of possible angles for the global input angle  $\beta$  is  $[0, 2\pi)$ . In this range of angles, the swarm assumes eight different polygonal shapes. The shapes alternate between triangles and trapezoids when the area  $A < 1/2$ , and alternate between squares with one corner removed and trapezoids when  $A > 1/2$ .

Computing the means, variances, covariance, and correlation requires integrating over the area containing the swarm. One way is to use an indicator function  $\mathbf{1}_A(x, y)$  that returns 1 if inside the region containing the swarm, and 0 else. The formulas for means  $(\bar{x}, \bar{y})$ , covariance  $(\sigma_x^2, \sigma_y^2, \sigma_{xy})$ , and

correlation  $\rho_{xy}$  are as follows, integrated over the unit square with  $x$  and  $y$  from 0 to 1:

$$\bar{x} = \frac{\iint x \mathbf{1}_A(x, y) dx dy}{A}, \quad \bar{y} = \frac{\iint y \mathbf{1}_A(x, y) dx dy}{A} \quad (1)$$

$$\sigma_x^2 = \frac{\iint (x - \bar{x})^2 \mathbf{1}_A(x, y) dx dy}{A}, \quad (2)$$

$$\sigma_y^2 = \frac{\iint (y - \bar{y})^2 \mathbf{1}_A(x, y) dx dy}{A} \quad (3)$$

$$\sigma_{xy} = \frac{\iint (x - \bar{x})(y - \bar{y}) \mathbf{1}_A(x, y) dx dy}{A}, \quad (4)$$

$$\rho_{xy} = \frac{\sigma_{xy}}{\sigma_x \sigma_y} \quad (5)$$

Rather than using an indicator function, the region of integration can be changed to only include the polygon containing the swarm. If the force angle is  $\beta$ , the mean when the swarm is in the lower-left corner is:

$$\begin{aligned} \bar{x}(A, \beta) &= \frac{\int_0^{\sqrt{2}\sqrt{-A \tan(\beta)}} \left( \int_0^{\sqrt{2}\sqrt{-A \cot(\beta) + x \cot(\beta)}} x dy \right) dx}{A} \\ &= \frac{1}{3} \sqrt{2} \sqrt{A \tan(\beta)} \end{aligned} \quad (6)$$

$$\begin{aligned} \bar{y}(A, \beta) &= \frac{\int_0^{\sqrt{2}\sqrt{-A \tan(\beta)}} \left( \int_0^{\sqrt{2}\sqrt{-A \cot(\beta) + x \cot(\beta)}} y dy \right) dx}{A} \\ &= \frac{1}{3} \sqrt{2} \sqrt{A \cot(\beta)} \end{aligned} \quad (7)$$

The full equations are included in the appendix, and are summarized in Fig. 2. A few highlights are that the correlation is maximized when the swarm is in a triangular shape, and is  $\pm 1/2$ . The covariance of triangle is always  $\pm(A/18)$ . Variance is maximized in one direction and minimized in the other when the swarm is in a rectangular shape. The range of mean positions are maximized when  $A$  is small.

d) *Circular workplace*: Though rectangular boundaries are common in artificial workspaces, biological workspaces are usually rounded. Similar calculations can be computed for a circular workplace. For notational simplicity, the swarm will be parameterized by the global control input signal  $\beta$  and the fill-level  $h$ , and the workspace is a circle centered at  $(0,0)$  with radius 1 and thus area  $\pi$ . In this case, the locus of mean positions are aligned with  $\beta$  and the mean position is at radius  $rad$  from the center. TODO...

#### B. Wall-Friction

Global inputs move a swarm uniformly. Controlling covariance requires breaking this uniform symmetry. A swarm inside an axis-aligned rectangular workspace can reduce variance normal to a wall by simply pushing the swarm into the boundary. Directly controlling covariance by pushing the swarm into a boundary requires changing the boundary. An obstacle in the lower-right corner is enough to generate positive covariance.

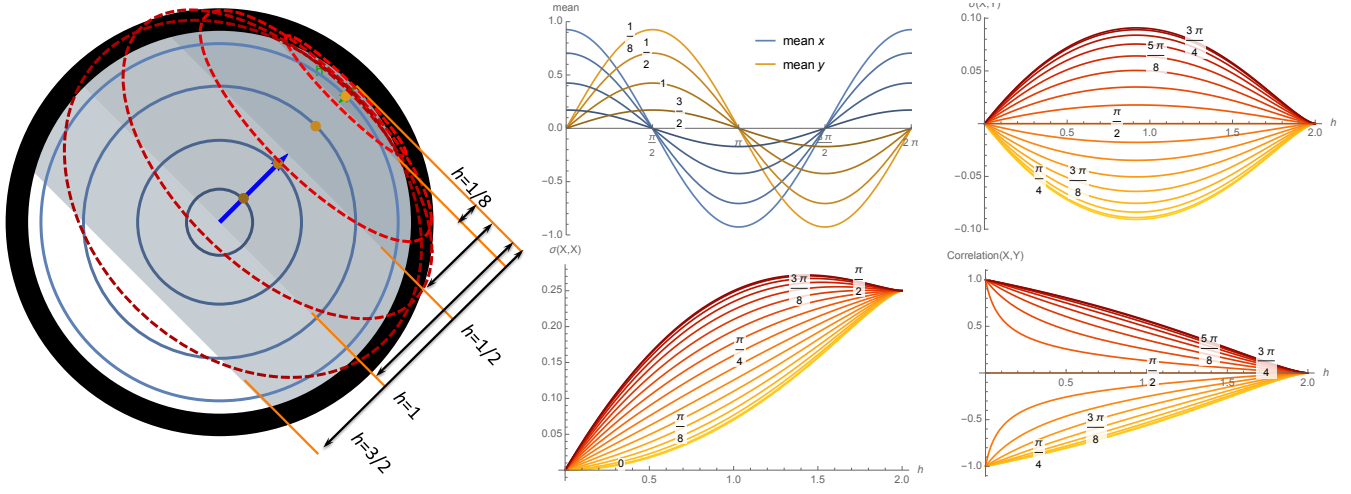


Fig. 2. Pushing the swarm against a circular boundary wall allows limited control of the shape of the swarm, as a function of the fill level  $h$  and the commanded movement direction  $\beta$ . The locus of possible mean positions are concentric circles. See interactive demonstration at [withheld for double-blind review].

Generating both positive and negative covariance requires additional obstacles. Requiring special obstacle configuration also makes covariance control dependent on the local environment. Instead of pushing our robots directly into a wall, this paper examines an oblique approach, by using boundaries that generate friction with the robots. These frictional forces are sufficient to break the symmetry caused by uniform inputs. Robots touching a wall have a negative friction force that opposes movement along the boundary, as shown in Eq. (8). This causes robots along the boundary to slow down compared to robots in free-space. This enables covariance control using boundaries with arbitrary orientations.

Let the control input be a vector force  $\vec{F}$  with magnitude  $F$  and orientation  $\theta$ .  $N$  is the normal or perpendicular force pushing the robot and the wall together. The force of friction  $F_f$  is

$$\begin{aligned} N &= F \cos(\theta) \\ F_f &= \begin{cases} \mu_f N, & \mu_f N < F \sin(\theta) \\ F \sin(\theta), & \text{else} \end{cases} \\ F_{\text{forward}} &= F \sin(\theta) - F_f \end{aligned} \quad (8)$$

Fig. 3 shows the resultant forces on two robots when one is touching a wall. As illustrated, both experiences different net forces although each receives the same inputs. For ease of analysis, the following algorithms assume  $\mu_f$  is infinite and robots touching the wall are prevented from sliding along the wall. This means that if one robot is touching the wall and another robot is free, if the control input is parallel or into the wall, the touching robot will not move. The next section shows how a system with friction model (8) and two walls are sufficient to arbitrarily position two robots.

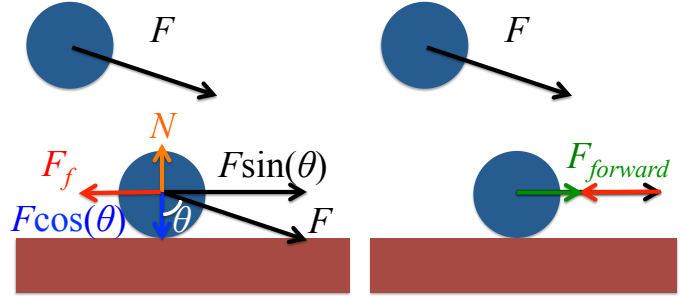


Fig. 3. Wall friction reduces the force for going forward  $F_{\text{forward}}$  on a robot near a wall, but not for a free robot.

### C. Position control of 2 robots using wall friction

This section describes an algorithm for positioning two robots and introduces concepts that will be used for multi-robot positioning. As we can see in Alg. 1, assume two robots are initialized at  $s_1$  and  $s_2$  with corresponding goal destinations  $e_1$  and  $e_2$ . Denote the current positions of the robots  $r_1$  and  $r_2$ . Let the subscripts  $x$  and  $y$  denote the  $x$  and  $y$  coordinates, i.e.,  $s_{1x}$  and  $s_{1y}$  denote the  $x$  and  $y$  locations of  $s_1$ . The algorithm assigns a global control input at every instance. As a result, our goal is to adjust  $\Delta r_x = r_{2x} - r_{1x}$  from  $\Delta s_x = s_{2x} - s_{1x}$  to  $\Delta e_x = e_{2x} - e_{1x}$  and similarly adjust  $\Delta r_y = r_{2y} - r_{1y}$  from  $\Delta s_y = s_{2y} - s_{1y}$  to  $\Delta e_y = e_{2y} - e_{1y}$  with one global input at every instance. The key to the algorithm is the position-dependent friction model (8).

Our algorithm uses a divide and conquer method to solve the positioning problem. It finds the final position of the robots in two steps: (i) First,  $|\Delta r_x - \Delta e_x|$  is reduced to zero while  $\Delta r_y$  is kept constant in Alg. 2. (ii) Having fixed  $\Delta r_x$  to  $\Delta e_x$

as desired, the algorithm next keeps  $\Delta r_x$  constant and adjusts  $\Delta r_y$  to  $\Delta e_y$ , as desired in Alg. 3. Though steps (i) and (ii) are similar from an algorithmic point of view, the following subsections describe the process in detail.

Step (i): Fixing  $\Delta r_x$

- Define  $e'_1 = (e_{1x}, s_{1y})$  and  $e'_2 = (e_{2x}, s_{2y})$ . Our goal for defining  $e'_1$  and  $e'_2$  is to understand the direction to which robots should move in order to adjust  $\Delta r_x$ . Let  $e'_{\text{top}} = \arg \max_i e'_{iy}$  and  $e'_{\text{bottom}} = \arg \min_i e'_{iy}$ . Now if  $e'_{\text{top},x} - e'_{\text{bottom},x} > 0$ , then the global input to both robots would be toward left direction and if  $e'_{\text{top},x} - e'_{\text{bottom},x} < 0$ , then the global input to both robots would be toward right direction. The two robots continue their horizontal path until one of them reaches the  $\epsilon$ -neighborhood of one of the left or right walls.
- At this step, let  $y_{\min} = \min_i r_{iy}$ , i.e.,  $y_{\min}$  is the minimum height of the two robots. We move both robots downward by the amount of  $y_{\min}$  such that one of the robots would touch the bottom wall and hence friction force will not let that robot to move left or right.
- The fact that the friction force of the bottom wall would not let the lower robot to move right or left will let the other robot to move to right and left freely to adjust  $\Delta r_x$  according to  $\Delta e_x$ .
- Finally, even if with the free move of the upper robot  $\Delta r_x$  is not set to the  $\Delta e_x$ , we can run the Step (i) (as described in the previous paragraphs) again to adjust the  $\Delta r_x$ . It is easy to show that it is guaranteed that we can adjust  $\Delta r_x$  to  $\Delta e_x$  in only two iterations.

Step (ii): Fixing  $\Delta r_y$  Now that we have adjusted the difference in robots' positions along one axis, we focus to do the same on the other axis as well. Therefore, similar to Section III-C, we employ the following steps:

- Let  $s'_1$  and  $s'_2$  be the points we derived at the end of the steps in Section III-C.
- Define  $e''_1 = (s'_{1x}, e_{1y})$  and  $e''_2 = (s'_{2x}, e_{2y})$ . We define  $e''_1$  and  $e''_2$  to understand the direction to which robots should move in order to adjust  $\Delta r_y$ . Let  $e''_{\text{right}} = \arg \max_i e''_{ix}$  and  $e''_{\text{left}} = \arg \min_i e''_{ix}$ . Now if  $e''_{\text{right},y} - e''_{\text{left},y} > 0$ , then the global input to both robots would be toward down direction and if  $e''_{\text{right},y} - e''_{\text{left},y} < 0$ , then the global input to both robots would be toward up direction. The two robots continue their vertical path until one of them reaches the  $\epsilon$ -neighborhood of one of the top or bottom walls.
- At this step, let  $x_{\min} = \min_i r_{ix}$ , i.e.,  $x_{\min}$  is the minimum distance of the two robots from the origin along the  $x$ -axis. We move both robots to the left by the amount of  $x_{\min}$  such that one of the robots would touch the left wall and hence friction force will not let that robot to move up or down.
- The fact that the friction force of the left wall would not let one of the robots to move up or down will let the other robot to move to up or down freely to adjust  $\Delta r_y$  according to  $\Delta e_y$ .

- Finally, even if with the free move of the robot which is not touching the wall  $\Delta r_y$  is not set to the  $\Delta e_y$ , we can run the Step (i) (as described in the previous paragraphs) again to adjust the  $\Delta r_y$ . It is easy to show that it is guaranteed that we can adjust  $\Delta r_y$  to  $\Delta e_y$  in only two iterations.

Once  $\Delta r_x$  and  $\Delta r_y$  are set to  $\Delta e_x$  and  $\Delta e_y$ , we can use global input to easily move both robots from  $r_1$  and  $r_2$  toward  $e_1$  and  $e_2$ .

---

**Algorithm 1** WallFrictionArrange2Robots( $s_1, s_2, e_1, e_2, L$ )

---

**Require:** Knowledge of starting ( $s_1, s_2$ ) and ending ( $e_1, e_2$ ) positions of two robots. (0,0) is bottom corner,  $s_1$  is rightmost robot,  $L$  is length of the walls. Current position of the robots are ( $r_1, r_2$ ).

- 1: ( $r_1, r_2$ ) = GenerateDesiredx-spacing( $s_1, s_2, e_1, e_2, L$ )
  - 2: GenerateDesiredy-spacing( $r_1, r_2, e_1, e_2, L$ )
- 

---

**Algorithm 2** GenerateDesiredx-spacing( $s_1, s_2, e_1, e_2, L$ )

---

**Require:** Knowledge of starting ( $s_1, s_2$ ) and ending ( $e_1, e_2$ ) positions of two robots. (0,0) is bottom corner,  $s_1$  is topmost robot,  $L$  is length of the walls. Current robot positions are ( $r_1, r_2$ ).

**Ensure:**  $r_{1y} - r_{2y} \equiv s_{1y} - s_{2y}$

- 1:  $\epsilon \leftarrow$  small number
  - 2:  $\Delta s_x \leftarrow s_{1x} - s_{2x}$
  - 3:  $\Delta e_x \leftarrow e_{1x} - e_{2x}$
  - 4:  $r_1 \leftarrow s_1, r_2 \leftarrow s_2$
  - 5: **if**  $\Delta e_x < 0$  **then**
  - 6:    $m \leftarrow (L - \epsilon - \max(r_{1x}, r_{2x}), 0) \triangleright$  Move to right wall
  - 7: **else**
  - 8:    $m \leftarrow (\epsilon - \min(r_{1x}, r_{2x}), 0) \triangleright$  Move to left wall
  - 9: **end if**
  - 10:  $m \leftarrow m + (0, -\min(r_{1y}, r_{2y})) \triangleright$  Move to bottom
  - 11:  $r_1 \leftarrow r_1 + m, r_2 \leftarrow r_2 + m \triangleright$  Apply move
  - 12: **if**  $\Delta e_x - (r_{1x} - r_{2x}) > 0$  **then**
  - 13:    $m \leftarrow (\min(|\Delta e_x - \Delta s_x|, L - r_{1x}), 0) \triangleright$  Move right
  - 14: **else**
  - 15:    $m \leftarrow (-\min(|\Delta e_x - \Delta s_x|, r_{1x}), 0) \triangleright$  Move left
  - 16: **end if**
  - 17:  $m \leftarrow m + (0, \epsilon) \triangleright$  Move up
  - 18:  $r_1 \leftarrow r_1 + m, r_2 \leftarrow r_2 + m \triangleright$  Apply move
  - 19:  $\Delta r_x = r_{1x} - r_{2x}$
  - 20: **if**  $\Delta r_x \equiv \Delta e_x$  **then**
  - 21:   **return** ( $r_1, r_2$ )
  - 22: **else**
  - 23:   **return** GenerateDesiredx-spacing( $r_1, r_2, e_1, e_2, L$ )
  - 24: **end if**
- 

#### D. Position Control of $n$ robots using wall friction

Algorithm 1 can be extended to control the position of  $n$  robots using wall friction under several constraints. The solution described here is an iterative procedure with  $n$  loops.



---

**Algorithm 3** GenerateDesiredy-spacing( $s_1, s_2, e_1, e_2, L$ )

**Require:** Knowledge of starting ( $s_1, s_2$ ) and ending ( $e_1, e_2$ ) positions of two robots. (0,0) is bottom corner,  $s_1$  is rightmost robot,  $L$  is length of the walls. Current position of the robots are ( $r_1, r_2$ ).

**Ensure:**  $r_{1x} - r_{2x} \equiv s_{1x} - s_{2x}$

```
1:  $\Delta s_y \leftarrow s_{1y} - s_{2y}$ 
2:  $\Delta e_y \leftarrow e_{1y} - e_{2y}$ 
3:  $r_1 \leftarrow s_1, r_2 \leftarrow s_2$ 
4: if  $\Delta e_y < 0$  then
5:    $m \leftarrow (L - \max(r_{1y}, r_{2y}), 0)$   $\triangleright$  Move to top wall
6: else
7:    $m \leftarrow (-\min(r_{1y}, r_{2y}), 0)$   $\triangleright$  Move to bottom wall
8: end if
9:  $m \leftarrow m + (0, -\min(r_{1x}, r_{2x}))$   $\triangleright$  Move to left
10:  $r_1 \leftarrow r_1 + m, r_2 \leftarrow r_2 + m$   $\triangleright$  Apply move
11: if  $\Delta e_y - (r_{1y} - r_{2y}) > 0$  then
12:    $m \leftarrow (\min(|\Delta e_y - \Delta s_y|, L - r_{1y}), 0)$   $\triangleright$  Move top
13: else
14:    $m \leftarrow (-\min(|\Delta e_y - \Delta s_y|, r_{1y}), 0)$   $\triangleright$  Move bottom
15: end if
16:  $m \leftarrow m + (0, \epsilon)$   $\triangleright$  Move right
17:  $r_1 \leftarrow r_1 + m, r_2 \leftarrow r_2 + m$   $\triangleright$  Apply move
18:  $\Delta r_y = r_{1y} - r_{2y}$ 
19: if  $\Delta r_y \equiv \Delta e_y$  then
20:    $m \leftarrow (e_{1x} - r_{1x}, e_{1y} - r_{1y})$ 
21:    $r_1 \leftarrow r_1 + m, r_2 \leftarrow r_2 + m$   $\triangleright$  Apply move
22:   return ( $r_1, r_2$ )
23: else
24:   return GenerateDesiredy-spacing( $r_1, r_2, e_1, e_2, L$ )
25: end if
```

---

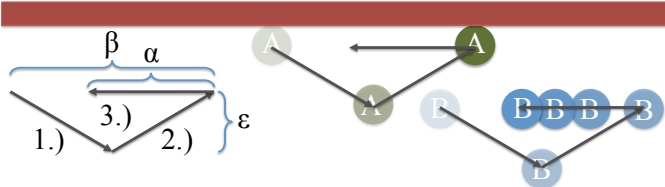


Fig. 4. A DriftMove( $\alpha, \beta, \epsilon$ ) to the right consists of repeating a triangular movement sequence  $\{(\beta/2, -\epsilon), (\beta/2, \epsilon), (-\alpha, 0)\}$ . The robot  $A$  touching a top wall will move right  $\beta$  units, while robots not touching the top move right  $\beta - \alpha$ .

The  $k$ th loop moves the  $k$ th robot from a *staging zone* to the desired position in a *build zone*. At the end the  $k$ th loop, robots 1 through  $k$  are in their desired final configuration in the build zone, and robots  $k + 1$  to  $n$  are in the staging zone.

Assume an open workspace with four axis-aligned walls with infinite friction. The axis-aligned build zone of dimension ( $w_b, h_b$ ) containing the final configuration of  $n$  robots must be disjoint from the axis-aligned staging zone of dimension ( $w_s, h_s$ ) containing the starting configuration of  $n$  robots. Without loss of generality, assume the build zone is above the staging zone. Furthermore, there must be at least  $\epsilon$

space above the build zone,  $\epsilon$  below the staging zone, and  $\epsilon + 2r$  to the left of the build and staging zone, where  $r$  is the radius of a robot. The minimum workspace is then  $(\epsilon + 2r + \max(w_f, w_s), 2\epsilon + h_s, h_f)$ .

The  $n$  robot position control algorithm relies on a DriftMove( $\alpha, \beta, \epsilon$ ) control input, shown in Fig. 4. A drift move consists of repeating a triangular movement sequence  $\{(\beta/2, -\epsilon), (\beta/2, \epsilon), (-\alpha, 0)\}$ . The robot touching a top wall moves right  $\beta$  units, while robots not touching the top move right  $\beta - \alpha$ .

Let (0,0) be the lower left corner of the workspace,  $p_k$  the  $x, y$  position of the  $k$ th robot, and  $f_k$  the final  $x, y$  position of the  $k$ th robot. Label the robots in the staging zone from left-to-right and top-to-bottom, and the  $f_k$  configurations right-to-left and top-to-bottom as shown in Fig. 5.

---

**Algorithm 4** PositionControlnRobotsUsingWallFriction( $k$ )

```
1: move( $-\epsilon, r - p_{k,y}$ )
2: while  $p_{k,x} > r$  do
3:   DriftMove(0,  $\min(p_{k,x} - r, \epsilon), \epsilon$ ) left
4: end while
5:  $m \leftarrow \text{ceil}(\frac{f_{k,y} - r}{\epsilon})$ 
6:  $\beta \leftarrow \frac{f_{k,y} - r}{m}$ 
7:  $\alpha \leftarrow \beta - \frac{r - p_{k,y} - \epsilon}{m}$ 
8: for  $m$  iterations do
9:   DriftMove( $\alpha, \beta, \epsilon$ ) up
10: end for
11: move( $r + \epsilon - f_{k,x}, 0$ )
12: move( $f_{k,x} - r, 0$ )
```

---

Alg. 4 proceeds as follows: First, the robots are moved left away from right wall, and down so robot  $k$  touches the bottom wall. Second, a set of DriftMove()s are executed that move robot  $k$  to the left wall with no net movement of the other robots. Third, a set of DriftMove()s are executed that move robot  $k$  to its target height and return the other robots to their initial heights. Fourth, all robots except robot  $k$  are pushed left until robot  $k$  is in the correct relative  $x$  position compared to robots 1 to  $k - 1$ .

Finally, all robots are moved right until robot  $k$  is in the desired target position.

### E. Controlling Covariance Using Wall Friction

We can use friction to control covariance of the swarm.

---

**Algorithm 5** Swarm Covariance Control With Wall Friction

**Require:** Swarm is Gaussian Distributed(in limit it is uniformly distributed)

**Require:**  $L$  is the length of the  $x$  of the workspace

```
1: while  $\text{dox} < L - \sigma_x(t)$ 
2:   Go Left
3: end while
4: Go Up for ...
```

---

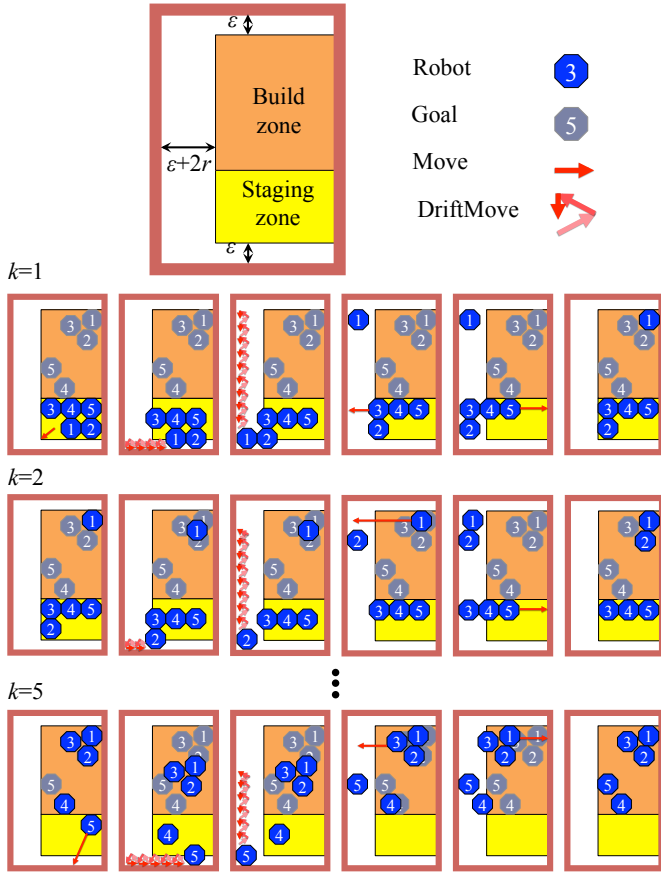


Fig. 5. Illustration of Alg. 4,  $n$  robot position control using wall friction.

#### IV. SIMULATION

Two simulations were implemented using wall-friction for position control. The first controls the position of two robots, the second controls the position of  $n$  robots. All code is available online at [link withheld for review].

TODO: should we also have simulated results with no friction? Simulated results of covariance control?

##### A. Position Control of Two Robots

Algorithms 1, 2, 3, were implemented in Mathematica using point robots (radius = 0). Figs 6 and ?? show the examples of the implementation of our algorithm. Robot initial positions are shown by a crosshair, and final positions by a circled crosshair. Dashed lines show the shortest route if robots could be controlled independently. The path given by Alg. 1 is shown with solid arrows.

In each of these figures we have five snapshots of the running of our algorithm taken every quarter second. For the sake of brevity we have replaced straight moves (e.g. upward, downward, etc) with oblique moves that shows a combination of two moves simultaneously (e.g. left and down together).

As we can see, in Fig. 6  $\Delta r_x$  is adjusted to  $\Delta e_x$  in the second snapshot, i.e., at  $t = t_1$  where  $t_1 < 0.25$ . The rest of the steps in this figure is dedicated to adjusting the  $\Delta r_y$  to  $\Delta e_y$ . As it is clear from Fig. 6,  $\Delta r_y$  is also adjusted at

$t = t_2$  where  $0.75 < t_2 < 1$ . Finally, once  $\Delta r_x$  and  $\Delta r_y$  are adjusted, the algorithm gives a global input both of the robots so as to move them toward their corresponding destinations. This is happening in the time interval of  $(t_2, 1]$ .

Similarly, in Fig. 6B we can see that the  $\Delta r_x$  is adjusted in the third snapshot, i.e., at  $t = t_3$  where  $0.25 < t_3 < 0.5$  and  $\Delta r_y$  is adjusted in the last snapshot at  $t = t_4$  where  $0.75 < t_4 < 1$ . The final positioning steps are happening in the time interval of  $(t_4, 1]$ .

As we pointed out earlier, adjusting each of  $\Delta r_x$  and  $\Delta r_y$  needs two iterations in the worst case. In other words, both of the Alg. 2 and Alg. 3 are executed two times in the worst case in positioning process of the robots. It is easy to see that we need two iterations of Alg. 2 only if  $|\Delta e_x - \Delta s_x| > L$ . Similarly we need two iterations of Alg. 3 only if  $|\Delta e_y - \Delta s_y| > L$ .

##### B. Position Control of $n$ Robots

ARUN'S part  
2 figures, discussion.

#### V. EXPERIMENT

##### A. Hardware system

Our experiments are on centimeter-scale hardware systems called *kilobots*. These allows us to emulate a variety of dynamics, while enabling a high degree of control over robot dynamics, the environment, and data collection. The kilobot Rubenstein et al. [10, 11] is a low-cost robot designed for testing collective algorithms with large numbers of robots. It is available commercially or as an open source platform K-Team [5]. Each robot is approximately 3 cm in diameter, 3 cm tall, and uses two vibration motors to move on a flat surface at speeds up to 1 cm/s. Each robot has one ambient light sensor that is used to implement *phototaxis*, moving towards a light source. In these experiments as shown in Fig. 7, we used  $n=64$  kilobots, a 1.5 m  $\times$  1.2 m whiteboard as the workspace, and four 30W LED floodlights arranged 1.5 m above the plane of the table at the  $\{N, E, S, W\}$  vertices of a 6 m square centered on the workspace. The lights were controlled using an Arduino Uno board connected to an 8 relay shield board. At top of the table, an overhead machine vision system was added to track the position of the swarm.

The walls of the hardware platform have almost infinite friction, due to the three legged design of the kilobots. When a kilobot is steered into the wall, they pin themselves to the wall until the light changes direction and they begin turning in the other direction. This wall friction is sufficient to enable independent position control of two kilobots, as shown in Fig. 8.

To demonstrate covariance control  $n = 64$  robots were placed on the workspace and manually steered with a single light source, using friction with the boundary walls to vary the covariance from -5000 to 10,000. The resulting covariance is plotted in Fig. 9, along with snapshots of the swarm.

describe  
the  
8  
lights

units?

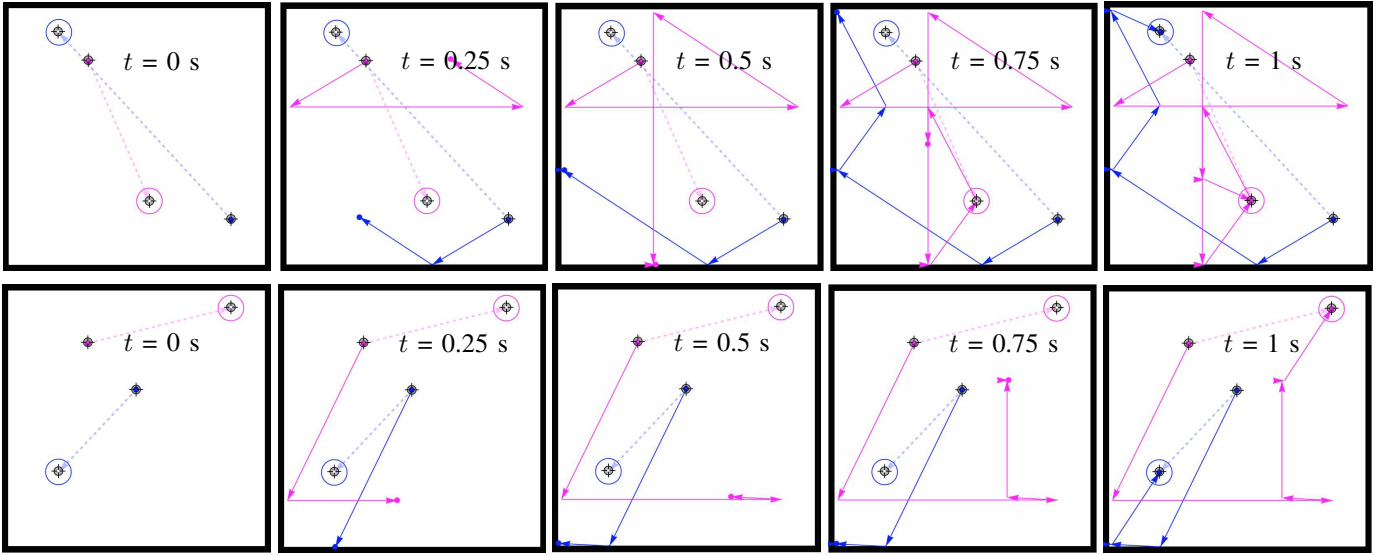


Fig. 6. Frames from an implementation of Alg. 1: two robot positioning using walls with infinite friction. Robot initial positions are shown by a crosshair, and final positions by a circled crosshair. Dashed lines show the shortest route if robots could be controlled independently. The path given by Alg. 1 is shown with solid arrows. The bottom row shows an extreme case where the robots must switch position.

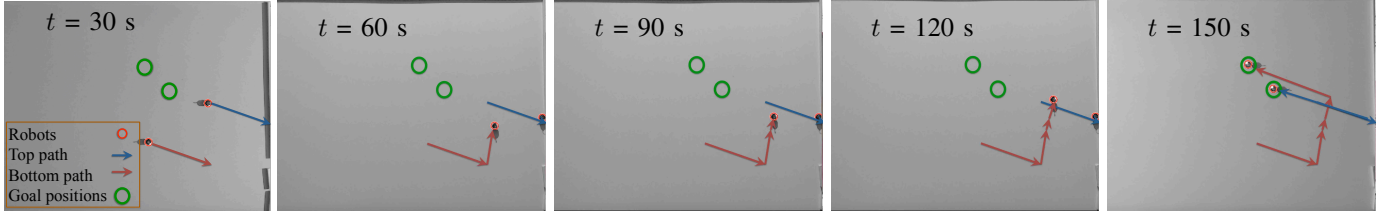


Fig. 8. Two robot positioning using the hardware setup and two kilobot robots. The walls have nearly infinite friction, as illustrated by this fig, the robot with the blue path that is stopped by the wall until the light changes orientation, while the orange robot in free-space is unhindered.

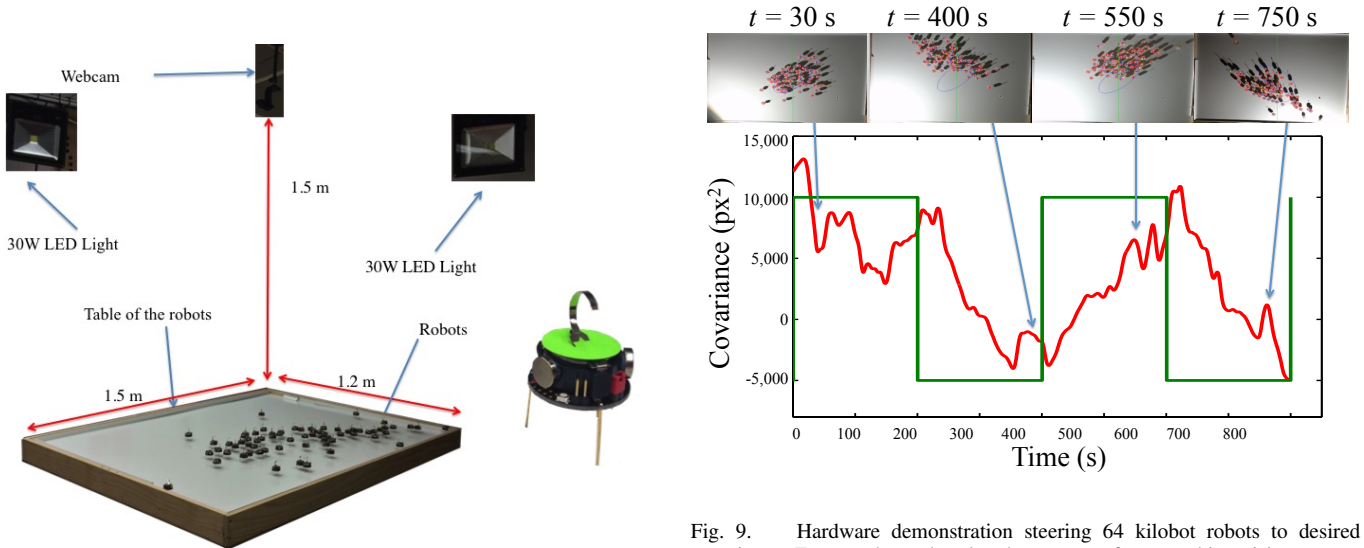


Fig. 9. Hardware demonstration steering 64 kilobot robots to desired covariance. Frames above the plot show output from machine vision system and an overlaid covariance ellipse.

Fig. 7. Hardware platform: table with  $1.5 \times 1.2$  m workspace, surrounded by eight remotely triggered 30W LED floodlights, with an overhead machine vision system.

## VI. CONCLUSION AND FUTURE WORK

This paper presented techniques for controlling the shape of a swarm of robots using global inputs and interaction with

boundary friction forces. The paper provided algorithms for precise position control, as well as demonstrations of efficient covariance control. Future efforts should be directed toward improving the technology and tailoring it to specific robot applications.

With regard to technological advances, this includes designing controllers that efficiently regulate  $\sigma_{xy}$ , perhaps using Lyapunov-inspired controllers as in Kim et al. [6]. Additionally, this paper assumed that wall friction was nearly infinite. The algorithms require retooling to handle small  $\mu_f$  friction coefficients. It may be possible to rank controllability as a function of friction. In hardware, friction could be modified by outfitting the kilobots with a round skirt to avoid the almost infinite friction due to the triangular leg arrangement. The wall friction can be varied by laser-cutting boundary walls with different of profiles.

#### ACKNOWLEDGMENTS

Withheld for double-blind review

#### REFERENCES

- [1] Bruce R Donald, Christopher G Levey, Igor Paprotny, and Daniela Rus. Planning and control for microassembly of structures composed of stress-engineered mems microrobots. *The International Journal of Robotics Research*, 32(2):218–246, 2013. URL <http://ijr.sagepub.com/content/32/2/218.abstract>.
- [2] Magnus Egerstedt and Xiaoming Hu. Formation constrained multi-agent control. *IEEE Trans. Robotics Automat.*, 17:947–951, 2001.
- [3] Ambarish Ghosh and Peer Fischer. Controlled propulsion of artificial magnetic nanostructured propellers. *Nano Letters*, 9(6):2243–2245, 2011/10/23 2009. doi: 10.1021/nl900186w. URL <http://dx.doi.org/10.1021/nl900186w>.
- [4] M Ani Hsieh, Vijay Kumar, and Luiz Chaimowicz. Decentralized controllers for shape generation with robotic swarms. *Robotica*, 26(05):691–701, 2008.
- [5] K-Team. Kilobot, [www.k-team.com/mobile-robotics-products/kilobot](http://www.k-team.com/mobile-robotics-products/kilobot), 2015.
- [6] Paul Seung Soo Kim, Aaron Becker, Yan Ou, Anak Agung Julius, and Min Jun Kim. Imparting magnetic dipole heterogeneity to internalized iron oxide nanoparticles for microorganism swarm control. *Journal of Nanoparticle Research*, 17(3):1–15, 2015.
- [7] Sylvain Martel. Magnetotactic bacteria for the manipulation and transport of micro-and nanometer-sized objects. *Micro-and Nanomanipulation Tools*, 2015.
- [8] Sylvain Martel, Samira Taherkhani, Maryam Tabrizian, Mahmood Mohammadi, Dominic de Lanauze, and Ouajdi Felfoul. Computer 3d controlled bacterial transports and aggregations of microbial adhered nano-components. *Journal of Micro-Bio Robotics*, 9(1-2):23–28, 2014.
- [9] Bruce R. Munson, Alric P. Rothmayer, Theodore H. Okiishi, and Wade W. Huebsch. *Fundamentals of Fluid Mechanics*. Wiley, 7 edition, 2012.
- [10] M. Rubenstein, C. Ahler, and R. Nagpal. Kilobot: A low cost scalable robot system for collective behaviors. In *IEEE Int. Conf. Rob. Aut.*, pages 3293–3298, May 2012.
- [11] Michael Rubenstein, Alejandro Cornejo, and Radhika Nagpal. Programmable self-assembly in a thousand-robot swarm. *Science*, 345(6198):795–799, 2014.
- [12] Diana Spears, Wesley Kerr, and William Spears. Physics-based robot swarms for coverage problems. *The international journal of intelligent control and systems*, 11(3), 2006.
- [13] A. Sudsang and L. E. Kavraki. A geometric approach to designing a programmable force field with a unique stable equilibrium for parts in the plane. In *Proceedings of The 2001 IEEE International Conference on Robotics and Automation (ICRA 2001)*, volume 2, pages 1079–1085, Seoul, Korea, May 2001. IEEE Press, IEEE Press. doi: 10.1109/ROBOT.2001.932737. This paper was a finalist for best conference paper award.
- [14] T.H. Vose, P. Umbanhowar, and K.M. Lynch. Friction-induced velocity fields for point parts sliding on a rigid oscillated plate. *The International Journal of Robotics Research*, 28(8):1020–1039, 2009. doi: 10.1177/0278364909340279. URL <http://ijr.sagepub.com/content/28/8/1020.abstract>.
- [15] Thomas H Vose, Paul Umbanhowar, and Kevin M Lynch. Sliding manipulation of rigid bodies on a controlled 6-dof plate. *The International Journal of Robotics Research*, 31(7):819–838, 2012.
- [16] Xiaohui Yan, Qi Zhou, Jiangfan Yu, Tiantian Xu, Yan Deng, Tao Tang, Qian Feng, Liming Bian, Yan Zhang, Antoine Ferreira, and Li Zhang. Magnetite nanostructured porous hollow helical microswimmers for targeted delivery. *Advanced Functional Materials*, 25(33):5333–5342, 2015. ISSN 1616-3028. doi: 10.1002/adfm.201502248. URL <http://dx.doi.org/10.1002/adfm.201502248>.